ARTICLE IN PRESS

Journal of Contaminant Hydrology xxx (xxxx) xxx–xxx

Contents lists available at ScienceDirect

Journal of Contaminant Hydrology

journal homepage: www.elsevier.com/locate/jconhyd

Visualization and simulation of density driven convection in porous media using magnetic resonance imaging

James A. Montague[a,*], George F. Pinder[a], Jay V. Gonyea[b], Scott Hipko[b], Richard Watts[b]

[a] Civil and Environmental Engineering, University of Vermont, Burlington, VT, USA
[b] Department of Radiology, University of Vermont College of Medicine, Burlington, VT, USA

A R T I C L E I N F O

Keywords:
Magnetic resonance imaging
Porous media
Numerical modeling
Density driven convection

A B S T R A C T

Magnetic resonance imaging is used to observe solute transport in a 40 cm long, 26 cm diameter sand column that contained a central core of low permeability silica surrounded by higher permeability well-sorted sand. Low concentrations (2.9 g/L) of Magnevist, a gadolinium based contrast agent, produce density driven convection within the column when it starts in an unstable state. The unstable state, for this experiment, exists when higher density contrast agent is present above the lower density water. We implement a numerical model in OpenFOAM to reproduce the observed fluid flow and transport from a density difference of 0.3%. The experimental results demonstrate the usefulness of magnetic resonance imaging in observing three-dimensional gravity-driven convective-dispersive transport behaviors in medium scale experiments.

1. Introduction

Small differences in fluid density create complex fluid flow paths. These complex flow paths enhance fluid mixing and therefore dispersive transport. We visualize the concentration resulting from these complex flow paths using magnetic resonance imaging (MRI).

1.1. Density driven convection in carbon capture and storage

An important problem wherein density driven convection plays a role is carbon capture and storage (CCS). This is because convection decreases the dissolution time of CO_2 in deep saline aquifers. Supercritical CO_2 injected into saline aquifers will rise to the top from the positive buoyancy of CO_2. Over time, CO_2 slowly dissolves into the top layers of brine, increasing its density (IPCC, 2005). The density increase in the top layer relative to the brine below gives rise to unstable gravity driven flow. Fingering develops as local convection moves denser CO_2 saturated brine downward and replaces it with the less dense brine. This phenomenon has been observed at laboratory scales in two-dimensional Hele-Shaw cells (Faisal et al., 2013; Kneafsey and Pruess, 2009).

Kneafsey and Pruess (2009) used a Hele-Shaw cell and the tracer bromocresol green to show experimentally that density-driven convection was occurring with fluid density differences ranging between 0.1% and 1%. Faisal et al. (2013) expanded upon this work by varying the "permeability" of the Hele-Shaw cell by changing the width of the gap between the two glass plates. The variation in "permeability" showed that small changes greatly affected the time for fingering to reach the bottom of the cell.

1.2. NMR measurements in porous media

Nuclear magnetic resonance (NMR) has been used for non-invasive imaging of the structure of porous media. Issa and Mansfield (1994) used T_1 weighted images to estimate permeability in sandstones using the relationship between the T_1 of porous media and the T_1 of water. Komlosh et al. (2011) determined the average porosity of glass capillary tubes on the voxel scale (three-dimensional volume over which measurements are averaged) using double pulsed-field gradient diffusion weighted MRI. Saturation curves for various porous materials as was calculated by Muir et al. (2014) using T_2 mapping Spin Echo Single Point Imaging as water was displaced by heavy water.

NMR has also been used to measure flow through porous media in small-scale experiments. Shattuck et al. (1995) measured thermal convection patterns using a spin echo technique in a small cylinder packed with monodisperse plastic beads. Kimmich et al. (2001) used NMR to map fluid velocities in percolation clusters created with a circuit board plotter. Khrapitchev et al. (2002) tracked the locations of particles in a small porous media column using velocity exchange spectroscopy to examine the dispersive flow within a column. This NMR method allowed them to track molecules by applying a spin and observing their displacement after a small delay in a 10 mm diameter

* Corresponding author at: Civil and Environmental Engineering, University of Vermont, 33 Colchester Ave, Burlington, VT 05405, USA.
E-mail address: james.montague@uvm.edu (J.A. Montague).

http://dx.doi.org/10.1016/j.jconhyd.2017.07.005
Received 14 February 2017; Received in revised form 26 May 2017; Accepted 24 July 2017
0169-7722/

column. Seymour and Callaghan (1997) provide a good overview of the NMR methods used to image fluid flow in porous media.

In addition to mapping physical properties of porous media, the concentrations of magnetic tracers such as Gd-diethylene-triaminepentaacetate ($Gd\text{-}DTPA^{2-}$) can be tracked through time. Haber-Pohlmeier et al. (2010) demonstrated that $Gd\text{-}DTPA^{2-}$ can be tracked within a sand column in a MRI scanner to determine flow and transport behaviors in three-dimensions.

Contrast agents are required to be compounds that change the relaxivity of the solution in which they are dissolved; alternative contrast agents include $NiCl_2$ (Pearl et al., 1993) and $CuSO_4$ (Greiner et al., 1997). Greiner et al. (1997) packed two small columns with glass beads and calculated the concentration of copper sulfate at the outlet with both MRI and atomic absorption spectroscopy. The results for both homogeneous and heterogeneous bead packing showed that MRI was able to accurately measure outflow breakthrough curves with the added benefit of quantifying the concentration within the column.

2. Materials and methods

This work extends that of earlier research by focusing on the impact of low dye concentrations on gravity-driven convective-dispersive transport. More specifically, we use an intermediate scale physical model in conjunction with MRI and numerical modeling to visualize and evaluate the impact of gravity on porous-medium transport.

2.1. Experimental set up

The sand column employed in this work is designed to evaluate the impact of sharp interfaces on solute transport in porous media. The dimensions of the column are designed specifically to make use of the maximum field of view of the MRI Center for Biomedical Imaging's Philips 3T Achieva TX scanner located in the University of Vermont Medical Center. The scanner has a bore size of 60 cm and a usable volume diameter of 50 cm. Whole-body scanners are desirable for this study because they allow macroscopic flow to be captured over a large volume (Fukushima, 1999). Larger experiments also facilitate observation of scale-dependent behavior and limits the impact of column-wall boundary interactions on the experiment. A smaller magnet in either a horizontal or vertical configuration would allow for higher resolution concentration maps, but would suffer from limiting the size of soil strata used.

The column is packed with a centrally located cylinder of ground silica with a mean grain diameter of 10 µm. This cylinder is surrounded by clean Ottawa sand with a mean grain diameter of 200 µm. To realize this arrangement, the ground silica is first placed in a cylindrical sleeve, saturated, and frozen. A Shelby tube is used as the sleeve to freeze the silica for this experiment. This allows for easy extraction using a Shelby tube extractor. The fine silica cylinder is then cut to length and placed into the center of the large column. The annulus between the frozen silica is then filled with the clean Ottawa sand. After thawing, a sharp interface exists between the silica and the sand.

The basic schematic of the column is shown in Fig. 1. The column is built entirely out of plastic to allow safe imaging by the scanner. The presence of metallic objects or particles disrupts the magnetic field, resulting in signal loss, because MRI relies on a highly homogeneous magnetic field, both macroscopically and microscopically. Consequently, considerable effort has been taken to reduce the number of magnetic particles within our porous media by screening the sand with a strong neodymium magnet.

2.2. MRI scans

MRI uses the nuclear magnetic resonance signal from protons (hydrogen nuclei), in this case in water. The characteristic magnetic relaxation time of the longitudinal magnetization, T_1, depends on the

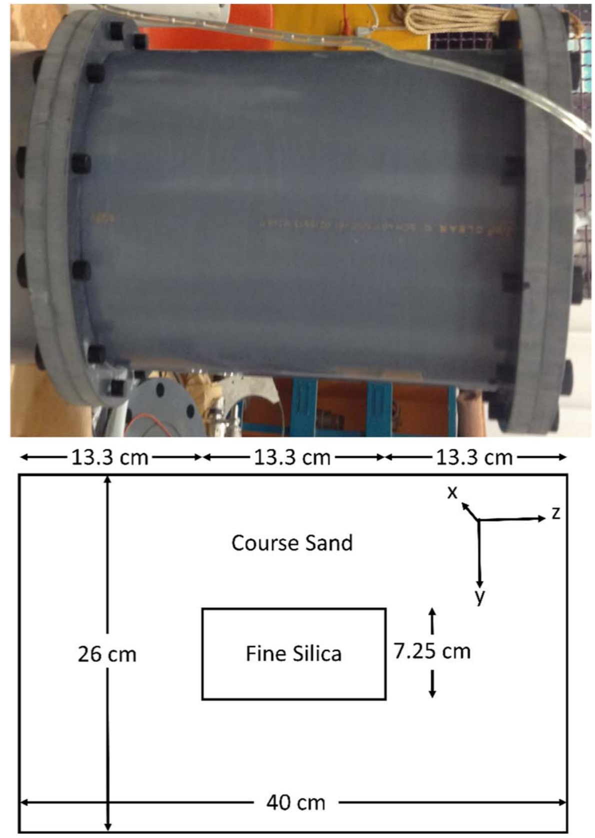

Fig. 1. As built schematic of the plastic sand column.

intrinsic relaxation time of water in the medium, T_{10}, and the concentration of magnetic materials including the gadolinium-based contrast agent used in this study. The relaxation time is related to the contrast concentration by Eq. (1),

$$\frac{c}{M} = \left(\frac{1}{T_1} - \frac{1}{T_{1back}}\right) \Big/ r_i \tag{1}$$

where c is the concentration of contrast agent in g/L in the saturated porous media, M is the molecular weight of the contrast in g/mmol. The variable T_{1back} is the background T_1 value of the porous media with distilled water in s^{-1}, and must be subtracted from the measured T_1 to remove the effects of different media on the measured signal. The variable r_i is the relaxivity of the contrast agent; for the case of Magnevist, r_i is 4.1 L/mmol·s based on empirical results (Tofts, 2010).

The spatial distribution of T_1 values can be calculated using various techniques. The spin-echo inversion recovery technique was used for this study. The recovery of longitudinal magnetization following inversion using a 180-degree RF pulse is described as an exponential function of the time between the inversion and the data acquisition (the inversion time, TI). It is given by Eq. (2),

$$M_z = M_0(1 - 2e^{-TI/T_1}) \tag{2}$$

where M_z is the longitudinal magnetization, M_0 is the maximum magnetization, TI is the inversion time, and T_1 is the unique value that describes the magnetic properties of each voxel.

Following the inversion time, TI, imaging data is acquired using a spin echo acquisition, resulting in an image in which the signal at each voxel is directly proportional to $M_z(TI)$. Note that this equation is based on the assumption of full recovery of magnetization between measurements, such that the repetition time $TR >> TI$. This assumption may not be justified for zero or very low concentrations of contrast agent, thus introducing a small bias in these cases.

Images are acquired with different values of inversion time, TI.